GAZE SHIFTS AS DYNAMICAL RANDOM SAMPLING

Giuseppe Boccignone

Dipartimento di Scienze dell'Informazione
Universitá di Milano
Via Comelico 39/41
20135 Milano, Italy
boccignone@dsi.unimi.it

Mario Ferraro

Dipartimento di Fisica Sperimentale
Universitá di Torino
via Pietro Giuria 1
10125 Torino, Italy
ferraro@ph.unito.it

ABSTRACT

We discuss how gaze behavior of an observer can be simulated as a Monte Carlo sampling of a distribution obtained from the saliency map of the observed image. To such end we propose the Levy Hybrid Monte Carlo algorithm, a dynamic Monte Carlo method in which the walk on the distribution landscape is modelled through Levy flights. Some preliminary results are presented comparing with data gathered by eye-tracking human observers involved in an emotion recognition task from facial expression displays.

Index Terms— Gaze analysis, Active vision, Hybrid Monte Carlo, Levy flights

1. INTRODUCTION

Vision is the dominant perceptual channel through which we interact with information and communication systems, but one major limitation of our visual communication capabilities is that we can attend to only a very limited number of features and events at any one time. This fact has severe consequences for visual communication, because what is effectively communicated depends to a large degree on those mechanisms in the brain that deploy our attentional resources and determine where we direct our gaze. Future ICT systems (dealing with gaze-contingent displays, attentive user interfaces, gaze-based interaction techniques, security systems, multimodal interfaces, augmented and mixed reality systems) should use gaze guidance to help the users deploy their limited attentional resources more effectively.

Gaze shifts are eye movements that play an important role: the Human Visual System (HVS) achieves highest resolution in the fovea - the small (about 1 degree of visual angle) central area of the retina- and the succession of rapid eye movements (saccades) compensates the loss of visual acuity in the periphery when looking at an object or a scene that spans more than several degrees in the observer's field of view. Thus, the brain directs saccades to actively reposition the center of gaze on circumscribed regions of interest, the so called "focus of attention" (FOA), to extract detailed information from the visual environment. An average of three eye fixations per second generally occurs, intercalated by saccades, during which vision is suppressed. The succession of gaze shifts is referred to as a scanpath [1].

Beyond the field of computational vision,[2], [3],[4], [5] and robotics [6], [7], much research has been performed in the image/video coding [8], [9]. [10], [11] , [12], and image/video retrieval domains [13],[14].

However, one issue which is not addressed by most models [15] is the "noisy", idiosyncratic variation of the random exploration exhibited by different observers when viewing the same scene, or even by the same subject along different trials [16] (see Fig. 1).

Fig. 1. Different gaze behaviors exhibited by four subjects involved in an emotion recognition task from facial expression. Circles represent fixations, straight lines the gaze-shifts.

Such results speak of the stochastic nature of scanpaths. Indeed, at the most general level one can assume any scanpath

to be the result of a random walk performed to visually sample the environment under the constraints of both the physical information provided by the stimuli (saliency or conspicuity) and the internal state of the observer, shaped by cognitive (goals, task being involved) and emotional factors.

Under this assumption, the very issue is how to model such "biased" random walk. In a seminal paper [17], Brockmann and Geisel have shown that a visual system producing Levy flights implements an efficient strategy of shifting gaze in a random visual environment than any strategy employing a typical scale in gaze shift magnitudes.

Levy flights provide a model of diffusion characterized by the occurrence of long jumps interleaved with local walk. In Levy flights the probability of a $|\xi|$-length jump is "broad", in that, asymptotically, $p(\xi) \sim |\xi|^{-1-\alpha}$, $0 < \alpha < 2$, whereas when $\alpha \geq 2$ normal (Gaussian) diffusion takes place [18].

To fully exploit diffusion dynamics, in [19], a gaze-shift model (the Constrained Levy Exploration, CLE) was proposed where the scanpath is guided by a Langevin equation,

$$\frac{d}{dt}\mathbf{x} = -U(\mathbf{x}) + \xi, \tag{1}$$

on a potential $U(\mathbf{x})$ modelled as a function of the saliency (landscape) and where the stochastic component $\xi \sim L_\alpha(\xi)$ represents random flights sampled from a Levy distribution (refer to [19] for a detailed discussion, and to [20],[21] for application to robot vision relying on Stochastic Attention Selection mechanisms). The basic assumption was the "foraging metaphor", namely that Levy-like diffusive property of scanpath behavior mirrors Levy-like patterns of foraging behavior in many animal species [22]. In this perspective, the Levy flight, as opposed, for instance, to Gaussian walk, is assumed to be essential for optimal search, where optimality is related to efficiency, that is the ratio of the number of sites visited to the total distance traversed by forager [22]. An example depicting the difference between Gaussian and Levy walks is provided in Fig. 1.

In this note we present a new method, the Levy Hybrid Monte Carlo (LHMC) algorithm, in which gaze exploration is obtained as a sampling sequence generated via a dynamic Monte Carlo technique [24]: here, in contrast with what is usually done, the stochastic element is given by a vector ξ sampled from a Levy distribution.

This perspective suggests a different and intriguing view of the saccadic mechanism: that of a motor system implementation of an active random sampling strategy that the HVS has evolved in order to efficiently and effectively infer properties of the surrounding world.

2. GAZE-SHIFT MODELING VIA LHMC

2.1. Background

Hybrid Monte Carlo (HMC) is a Markov chain Monte Carlo (MCMC) technique built upon the basic principle of Hamiltonian mechanics [24]. Suppose we wish to draw Monte Carlo samples from probability $p(\mathbf{x})$, $\mathbf{x} = \{x_i\}_{i=1}^N$. For many systems,

$$p(\mathbf{x}) = \frac{\exp(-U(\mathbf{x}))}{Z}, \tag{2}$$

where, in analogy to physical systems, $\mathbf{x}$ can be regarded as a position vector and $U(\mathbf{x})$ is the *potential energy* function. In a probabilistic context

$$U(\mathbf{x}) = \log \mathcal{L}(\mathbf{x}, \theta), \tag{3}$$

is the log-likelihood function.

By introducing an independent extra set of momentum variables $\mathbf{p} = \{p_i\}_{i=1}^N$ with i.i.d. standard Gaussian distributions we can add a kinetic term to the potential to produce a full Hamiltonian (energy) function on a fictitious phase-space,

$$H(\mathbf{x}, \mathbf{p}) = U(\mathbf{x}) + K(\mathbf{p}), \tag{4}$$

where $K(\mathbf{p}) = \frac{1}{2}\sum_i p_i^2$ is a *kinetic energy* and $U(\mathbf{x})$ is given by Eq. 3.

The canonical distribution associated to this Hamiltonian is :

$$p(\mathbf{x}, \mathbf{p}) = \frac{1}{Z_H} \exp\{-H(\mathbf{x}, \mathbf{p})\} \tag{5}$$

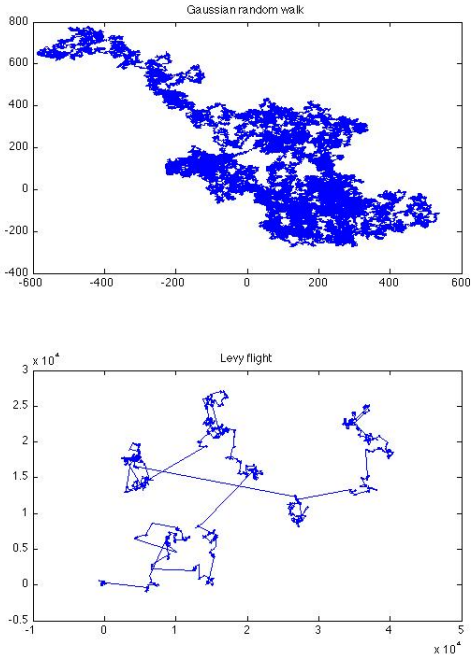

Fig. 2. Different walk patterns obtained through the method described in [23] (defined in the next section) . Top: Gaussian walk ($\alpha = 2$); bottom: Levy walk ($\alpha = 1.2$).

By comparing to Eq. 2, it is readily seen that $p(\mathbf{x}) = \sum_{\mathbf{p}} p(\mathbf{x}, \mathbf{p})$ is the marginal of the canonical distribution.

We can sample from $p(\mathbf{x}, \mathbf{p})$ by using a combination of Gibbs and Metropolis, and this density being separable, we can discard the momentum variables and retain only the sequence of position samples $\{\mathbf{x}_{t=1}, \mathbf{x}_{t=2}, \cdots\}$ that asymptotically come from the desired marginal distribution $p(\mathbf{x}) = \frac{\exp(-U(\mathbf{x}))}{Z}$.

Under the assumption that such physical system conserves the total energy (i.e. $H = const$), then its evolution dynamics can be described by the Hamiltonian equations:

$$\frac{d\mathbf{x}}{d\tau} = \dot{\mathbf{x}} = \frac{\partial H}{\partial \mathbf{p}} = \mathbf{p} \tag{6}$$

$$\frac{d\mathbf{p}}{d\tau} = \dot{\mathbf{p}} = -\frac{\partial H}{\partial \mathbf{x}} = \frac{\partial \log \mathcal{L}(\mathbf{x}, \theta)}{\partial \mathbf{x}} \tag{7}$$

where τ is a fictitious time along which we assume the system is evolving. Each iteration of the algorithm starts with a Gibbs sampling to pick a new momentum vector $\mathbf{p}$ from the Gaussian density $\frac{1}{Z_K} \exp\{-K(\mathbf{p})$, which is always accepted. Then the momentum variable determines where $\mathbf{x}$ goes in accordance with Eqs. 6 and 7

In practice, to simulate the Hamiltonian dynamics we need to discretize the equations of motion and in general, unless we are careful, the error introduced by the discretization destroys time reversibility and the preservation of volumes which are both needed for Metropolis to work without changes. The so called *leapfrog discretization* has the desired properties. A single leapfrog iteration updates the coordinates x_i, p_i in three sub-steps.

$$\hat{p}_i(\tau + \epsilon/2) = \hat{p}_i(\tau) - \frac{\epsilon}{2} \frac{\partial \log \mathcal{L}}{\partial x_i}(\hat{x}(\tau)), \tag{8}$$

$$\hat{x}_i(\tau + \epsilon) = \hat{x}_i(\tau) + \epsilon \hat{p}_i(\tau + \epsilon/2), \tag{9}$$

$$\hat{p}_i(\tau + \epsilon) = \hat{p}_i(\tau + \epsilon/2) - \frac{\epsilon}{2} \frac{\partial \log \mathcal{L}}{\partial x_i}(\hat{x}(\tau + \epsilon)). \tag{10}$$

Notice that in this fictitious dynamics the field of forces is supplied by the score function, i.e. the gradient of the log-likelihood.

In sum, the HMC algorithm operate as follows: 1) A direction λ for the trajectory is chosen ($\lambda = 1$ and $\lambda = -1$, representing forward and backward trajectories); 2) Starting from the current state $(\mathbf{x}, \mathbf{p})$, perform L leapfrog iterations with step size of $\epsilon = \lambda\epsilon_0$, reaching a new configuration $(\mathbf{x}^{'}, \mathbf{p}^{'}) = (\mathbf{x}(\epsilon L), \mathbf{p}(\epsilon L))$ in the phase space; 3) Accept $(\mathbf{x}^{'}, \mathbf{p}^{'})$ with probability $\min\{1, \exp[-(H(\mathbf{x}^{'}, \mathbf{p}^{'}) - H(\mathbf{x}, \mathbf{p}))\}$, otherwise keep the old state (Metropolis step).

The Metropolis step is introduced since the leapfrog discretization, although preserving volumes and being time reversible, no longer keeps $H = const$ (in fact it almost preserves H to order $O(\epsilon^2)$ giving rise to a small error $H' - H$). The value used for ϵ_0 is usually chosen at random from some fixed distribution.

2.2. Levy sampling via HMC

Note that if the number L of iterations of the leapfrog step is set to 1, then by taking into account Eqs. 8,9 and 10 the HMC method boils down to the Langevin Monte Carlo method where Eqs. 8,9 and 10 result in a single stochastic Langevin dynamics

$$\frac{d}{dt}\mathbf{x} = -\frac{\partial \log \mathcal{L}}{\partial \mathbf{x}}(\mathbf{x}) + \xi, \tag{11}$$

with $\xi \sim \mathcal{N}(0; 1)$.

This result can be generalized by assuming ξ to be an instance of Levy flights. As previously discussed, the motivation for introducing Levy distributions of flight lengths, as opposed, for instance, to Gaussian walk, is that such dynamics has be found to be be essential for optimal exploration in random searches [22].

Note that if a Levy distribution $L_\alpha(\xi)$ is used to sample the jump length ξ, then Eq.1 and thus the method described in [19] can be recovered as a special case.

Jumps $\xi_\alpha \sim L_\alpha(\xi)$ can be sampled in several ways [25] A well known method is the following by Chambers, Mallows, and Stuck [23]:

$$\xi_\alpha = \beta_x \left[\frac{-\log u \cos\phi}{\cos(1-\alpha)\phi}\right]^{1-1/\alpha} \frac{\sin(\alpha\phi)}{\cos\phi} \tag{12}$$

where $\phi = \pi(v - 1/2)$, $u, v \in (0, 1)$ are independent uniform random numbers, β_x is the scale parameter and ξ_α is a symmetric Levy α-stable random number.

3. EXPERIMENTS AND SIMULATION

Ten participants were required to observe 7 images, each representing a facial expression of a basic emotion (*anger, disgust, fear, happiness, sadness, surprise*) plus a neutral expression (placebo), in order to recognize the different expressions displayed. All had normal, or corrected to normal vision. Each face was viewed for 15 sec. Images extracted from the Cohn-Kanade dataset [26], served as stimuli.

Spurious features pertaining to the video were eliminated and the image size normalized to 462×600 pixels (width and height, respectively), thus subtending 9.11 deg. of visual angle horizontally and 11.83 deg. vertically at a viewing distance of 1 m, approximately equivalent to the size of a real face viewed from a distance of 1 m.

Eye movements were monitored with a SMI iView X Hi-Speed 1250 eye tracker offering a sampling rate of 1250 Hz. A bite-bar and forehead rest maintained the participant's viewing position and distance. Signals were sampled from the eye tracker, and raw data filtered to representative saccade and fixations via the SMI software

Since in this work, we are not concerned with deriving saliency maps (e.g., [2],[4]), but rather in the "motor" aspects of gaze behavior, such maps are derived via a 'reverse engineering' procedure from the cumulative fixations of all the

subjects in each facial expression (namely, the *fixation map*, [27]). Each image is partitioned in a fixed number of cells; the total number of fixations per cell by all subjects is counted, and a 2D Gaussian centered on each cell is multiplied by the counted value. The resulting matrix is normalized under the sum–to–one constraint and provides an estimate of the probability that a fixation is directed to each region, which in turn is directly related to the saliency of that region[27]. Fig. 3 shows the saliency/fixation maps for the different facial expressions.

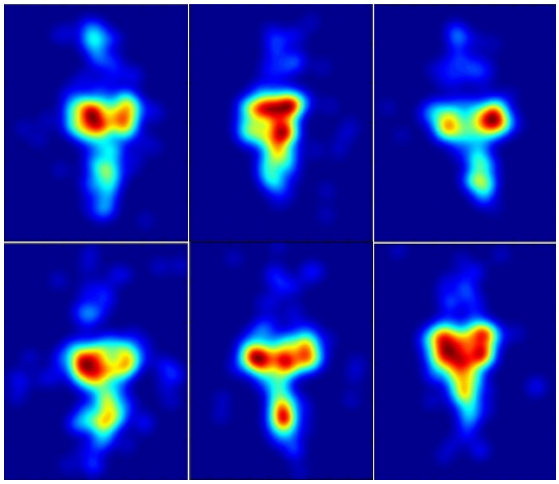

Fig. 3. Saliency maps obtained from eye-scanned subjects for six basic emotions. From top to bottom, left to right: anger, disgust, fear, joy, sadness, surprise

The results shown in Fig. 3 were somehow expected, since it is known that eye fixations tend to concentrate on eyes, nose and mouth regions during active visual perception of facial expressions [28].

Given the saliency maps for each emotional facial expressions, the potential energy function $U(\mathbf{x}) = \log \mathcal{L}(\mathbf{x}, \theta)$ is computed as the log-likelihood function of a mixture of Gaussians (MoG), which is used to fit each saliency map. The parameters of the MoG model are learned via the well known Expectation-Maximization algorithm. The number of mixture components has been set to 10, each component being a multivariate Gaussian of dimension 3 (the space coordinates $\mathbf{x}$ and the value of the saliency map at $\mathbf{x}$).

An example representative of the results obtained is presented in Fig. 3, right column. The saccadic walk is produced by the LHMC algorithm by setting $L = 40$ and retaining 1000 samples for each scanpath. Jumps $\xi_\alpha \sim L_\alpha(\xi)$ were sampled via Chambers, Mallows, and Stuck method [23]

Under such set-up, the simulation goes as follows

1. Fit the saliency with a MoG model, compute $U(\mathbf{x})$ via Eq.3 and $\partial \log \mathcal{L}/\partial x_i$, and initialize $(\mathbf{x}, \mathbf{p})$ (see, [24] for discussion)
2. **for** N samples **do**:
   (a) Choose direction λ for the trajectory
   (b) Sample $\xi_\alpha \sim L_\alpha(\xi)$ via Eq. 12, and compute the walk step $\epsilon(\lambda, \epsilon_0, \xi_\alpha)$;
   (c) Make L leapfrog iterations via Eqs 8, 9, 10 reaching a new configuration $(\mathbf{x}^{'}, \mathbf{p}^{'}) = (\mathbf{x}(\epsilon L), \mathbf{p}(\epsilon L))$ in the phase space;
   (d) Metropolis step: accept $(\mathbf{x}^{'}, \mathbf{p}^{'})$ with probability $\min\{1, \exp[-(H(\mathbf{x}^{'}, \mathbf{p}^{'}) - H(\mathbf{x}, \mathbf{p}))\}$, otherwise keep the old state

In the end, momenta $\mathbf{p}$ are discarded, and the sequence of coordinate samples $\{\mathbf{x}^t\}_{t=1}^N$ will represent the scanpath.

When comparing the results of the simulation with human scanpaths (Fig. 3, left column) it should be kept in mind that the latter represents saccades and fixation events as filtered by the eye-tracking apparatus on the basis of raw data gathered by the system, while our paths may be considered as unfiltered raw data. Thus, for a fair comparison one should run a suitable fixation/saccade detection algorithm (e.g., Nystrom and Holmqvist [29]) on the raw gaze points.

It can be seen that the LHMC algorithm effectively samples from the MoG distribution representing the saliency map of the task, and the gaze behavior obtained resembles scanpaths exhibited by human observers in such a complex cognitive task. This has been also evaluated by performing on the simulated scanpaths the same reverse engineering procedure described above to obtain the LHMC fixation maps and compared to human fixation maps.

This result is due to the fact that the LHMC efficiently explores the energy landscape, and in particular the use of Levy jumps provides an optimal walking strategy.

4. CONCLUSION

We have assumed here that the saccadic mechanism could be considered as a motor system implementation of an active random sampling strategy and that the HVS has evolved in order to efficiently and effectively infer properties of the surrounding world. On this basis we have proposed the Levy Hybrid Monte Carlo algorithm, in which gaze exploration is obtained as a sampling sequence generated via a dynamic Monte Carlo technique [24], where the random walk is driven by Levy diffusion.

Modelling of gaze shifts through a Levy process over a saliency field can shed light to well known properties of saccadic eye movements and in particular on the random variations of the search process exhibited by different observers when viewing the same scene, or even by the same subject along different trials [16].

We have shown that under such general framework, the Constrained Levy Exploration algorithm [19] can be recovered as a special case. Comparing to [19], where sampling

is performed in the configuration space $\{\mathbf{x}\}$, the extra burden of enlarging the dimensions of the sampling space to a the phase-space $\{\mathbf{x}, \mathbf{p}\}$ may look like an efficiency loss, but there is of course a benefit associated to this procedure. What is gained by adding the momentum variables is a way to efficiently explore large regions of phase-space by simulating the Hamiltonian dynamics in fictitious time. By following the dynamical path in phase-space, through the Levy flights we can propose cadidate moves that are far away from the current state but that still have a substantial chance of being accepted.

The LHMC algorithm could be used in recent visual communication trends , such as foveated image/video coding and retrieval [8], [9]. [10], [11] , [12], [13],[14] or more traditional computer vision and robotics [20],[21]. Other applications of interest could involve scanpath simulation for quantitative evaluation and performance assessment [30].

However, beyond any kind of possible application, the present research make some points that address the close intertwining of cognition perception and motor behaviour in terms of stochastic diffusion [31] which is central for the ongoing debate in modern cognitive science.

5. REFERENCES

[1] D. Noton and L. Stark, "Scanpaths in eye movements during pattern perception," *Science*, vol. 171, no. 968, pp. 308–311, 1971.

[2] A. Torralba, "Contextual priming for object detection," *Int. J. of Comp. Vis.*, vol. 53, pp. 153–167, 2003.

[3] Y. Sun and R. Fisher, "Object-based visual attention for computer vision," *Artificial Intelligence*, vol. 146, pp. 77–123, 2003.

[4] L. Itti, C. Koch, and E. Niebur, "A model of saliency-based visual attention for rapid scene analysis," *IEEE Trans. Pattern Anal. Machine Intell.*, vol. 20, pp. 1254–1259, 1998.

[5] D.H. Ballard, "Animate vision," *Art. Intell.*, , no. 48, pp. 57–86, 1991.

[6] S. Frintrop and P. Jensfelt, "Attentional landmarks and active gaze control for visual SLAM," *IEEE Trans. Robotics*, vol. 24, no. 5, pp. 1054–1065, 2008.

[7] A. Carbone, A. Finzi, A. Orlandini, and F. Pirri, "Model-based control architecture for attentive robots in rescue scenarios," *Autonomous Robots*, vol. 24, no. 1, pp. 87–120, 2008.

[8] C.M. Privitera, M. Azzariti, Y.F. Ho, and L.W. Stark, "A comparative study of focused Jpeg compression, FJpeg," *Patt. Rec. Lett.*, vol. 23, no. 10, pp. 1119–1127, 2002.

[9] Z. Wang and A. C. Bovik, "Embedded foveation image coding," *IEEE Trans. Image Processing*, vol. 10, no. 10, pp. 1397–1410, 2001.

[10] L. Sanghoon and A. C. Bovik, "Fast algorithms for foveated video processing," *IEEE Trans. Circuits Syst. Video Technol.*, vol. 13, no. 2, pp. 149–162, Feb. 2003.

[11] L. Itti, "Automatic foveation for video compression using a neurobiological model of visual attention," *IEEE Trans. Image Processing*, vol. 13, no. 10, pp. 1304–1318, October 2004.

[12] G. Boccignone, A. Marcelli, P. Napoletano, G. Di Fiore, G. Iacovoni, and S. Morsa, "Bayesian integration of face and low-level cues for foveated video coding," *IEEE Trans. Circuits Syst. Video Technol.*, vol. 18, no. 12, pp. 1727–1740, 2008.

[13] G. Boccignone, A. Chianese, V. Moscato, and A. Picariello, "Foveated shot detection for video segmentation," *IEEE Trans. Circuits Syst. Video Technol.*, vol. 15, no. 3, pp. 365–377, 2005.

[14] G. Boccignone, A. Chianese, V. Moscato, and A. Picariello, "Context-sensitive queries for image retrieval in digital libraries," *J. of Int. Inf. Sys.*, vol. 31, no. 1, pp. 53–84, 2008.

[15] S.R. Ellis and L. Stark, "Statistical dependency in visual scanning," *Human Factors: The Journal of the Human Factors and Ergonomics Society*, vol. 28, no. 4, pp. 421–438, 1986.

[16] C. M. Privitera and L. W. Stark, "Algorithms for defining visual regions-of-interest: Comparison with eye fixations," *IEEE Trans. Pattern Anal. Machine Intell.*, vol. 22, no. 9, pp. 970–982, September 2000.

[17] D. Brockmann and T. Geisel, "The ecology of gaze shifts," *Neurocomputing*, vol. 32, no. 1, pp. 643–650, 2000.

[18] J.P. Bouchaud and A. Georges, "Anomalous diffusion in disordered media: statistical mechanisms, models and physical applications," *Physics reports*, vol. 195, pp. 127–293, 1990.

[19] G. Boccignone and M. Ferraro, "Modelling gaze shift as a constrained random walk," *Physica A: Statistical Mechanics and its Applications*, vol. 331, no. 1-2, pp. 207–218, 2004.

[20] H. Martinez, M. Lungarella, and R. Pfeifer, "Stochastic Extension to the Attention-Selection System for the iCub," *University of Zurich, Tech. Rep*, 2008.

[21] Y. Nagai, "From bottom-up visual attention to robot action learning," in *Proceedings of 8 IEEE International Conference on Development and Learning*. IEEE Press, 2009.

[22] GM Viswanathan, EP Raposo, and MGE da Luz, "Lévy flights and superdiffusion in the context of biological encounters and random searches," *Physics of Life Rev.*, vol. 5, no. 3, pp. 133–150, 2008.

[23] JM Chambers, CL Mallows, and BW Stuck, "A method for simulating stable random variables," *J. Am. Stat. Ass.*, vol. 71, no. 354, pp. 340–344, 1976.

[24] R.M. Neal, *Probabilistic inference using Markov chain Monte Carlo methods*, Department of Computer Science, University of Toronto, 1993.

[25] D. Fulger, E. Scalas, and G. Germano, "Monte Carlo simulation of uncoupled continuous-time random walks yielding a stochastic solution of the space-time fractional diffusion equation," *Physical Review E*, vol. 77, no. 2, pp. 21122, 2008.

[26] T. Kanade, J.F. Cohn, and Y. Tian, "Comprehensive database for facial expression analysis," in *Proc. 4th IEEE Int. Conf. AFGR*, 2000, p. 46.

[27] D.S. Wooding, MD Mugglestone, KJ Purdy, and AG Gale, "Eye movements of large populations: II. Deriving regions of interest, coverage, and similarity using fixation maps," *Behav. Res. Meth. Instr. and Comp.*, vol. 34, no. 4, pp. 518–528, 2002.

[28] J.N. Buchan, M. Paré, and K.G. Munhall, "Spatial statistics of gaze fixations during dynamic face processing," *Social Neuroscience*, vol. 2, no. 1, pp. 1–13, 2007.

[29] M. Nyström and K. Holmqvist, "An adaptive algorithm for fixation, saccade, and glissade detection in eyetracking data," *Behavior Research Methods*, vol. 42, no. 1, pp. 188, 2010.

[30] A.T. Duchowski, J. Driver, S. Jolaoso, W. Tan, B.N. Ramey, and A. Robbins, "Scanpath comparison revisited," in *Proceedings of the 2010 Symposium on Eye-Tracking Research & Applications*. ACM, 2010, pp. 219–226.

[31] E. Todorov, "General duality between optimal control and estimation," in *47th IEEE Conference on Decision and Control, 2008. CDC 2008*, 2008, pp. 4286–4292.

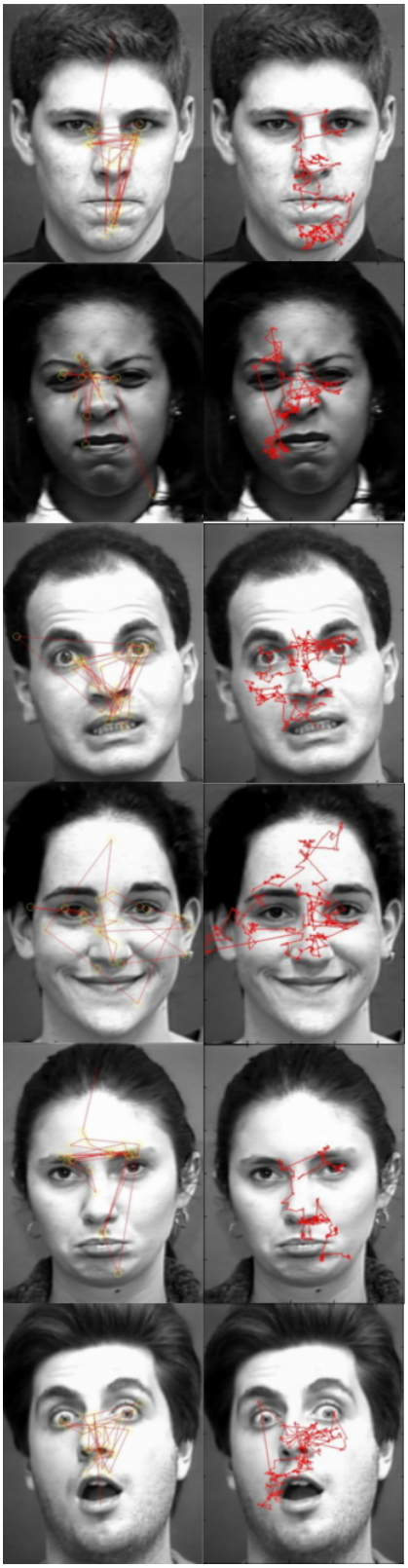

Fig. 4. Left column, gaze behavior of one subject, for different expressions; right column, scanpath simulated via the LHMC algorithm